

CsM₂Bi₃Te₆ and CsM₂Bi₃Te₇ (M = Pb, Sn): New Thermoelectric Compounds with Low-Dimensional Structures

Kuei-Fang Hsu,[†] Duck-Young Chung,[†] Sangeeta Lal,[‡] Antje Mrotzek,[†] Theodora Kyratsi,[†] Tim Hogan,[‡] and Mercouri G. Kanatzidis^{*†}

Department of Chemistry and Center for Fundamental Materials Research and Department of Electrical and Computer Engineering, Michigan State University, East Lansing, Michigan 48824

Received November 23, 2001

Progress in the field of thermoelectrics relies heavily on new materials and exploratory synthesis.¹ Low-dimensional structures are particularly attractive.² Once favorable new phases are discovered they become “platforms” for optimization through studies of solid solutions, nonstoichiometric compositions, and doping. In our laboratory the search for new thermoelectric materials is focused on ternary and quaternary bismuth chalcogenides. By virtue of their often complex anisotropic crystal and electronic structures, these materials can exhibit many essential features required for high figure of merit.^{3–11} A promising new phase that emerged is CsBi₄Te₆, which successfully reached a ZT of 0.8 at 225 K.¹² In an effort to produce new materials that resemble CsBi₄Te₆, we introduced Pb metal into its layered framework and searched for corresponding quaternary phases. This resulted in CsPbBi₃Te₆ (**1**) and CsPb₂Bi₃Te₇ (**2**), which were discovered through reactions of CsBi₄Te₆ with PbTe.^{13,14} Correspondingly the isostructural CsSnBi₃Te₆ (**3**) and CsSn₂Bi₃Te₇ (**4**) were obtained by reacting CsBi₄Te₆ with SnTe.^{15,16} The four compounds can also be prepared from stoichiometric mixtures of Cs₂Te, Pb (Sn), Bi, and Te. These phases adopt novel two-dimensional structures, reminiscent of but not the same as CsBi₄Te₆, built up of multilayered slabs. This family offers a brand-new quaternary system, Cs–M–Bi–Te (M = Pb and Sn), available for thermoelectric investigations, including fine-tuning of compositions and doping.

The layered structure of compound **1** consists of infinite anionic [PbBi₃Te₆][−] slabs separated with Cs⁺ cations, Figure 1a. Each [PbBi₃Te₆][−] slab consists of two crystallographically distinct metal sites, M(1) and M(2), both of which are octahedrally coordinated with Te atoms. Atoms Te(1), Te(2), and Te(3), are respectively 2-, 4-, and 6-coordinated with the metal atoms. The M–Te bond distances range between 2.964(2)–3.399(1) Å for M(1)Te₆ and 3.093(1)–3.231(1) Å for M(2)Te₆. The average M–Te distance is 3.173(1) Å, which is very similar to the average Bi–Te distance of 3.18 Å in CsBi₄Te₆. However, both MTe₆ octahedra in **1** have two short, two medium, and two long M–Te bonds. This behavior may be caused from the mixed Pb²⁺ and Bi³⁺ ion occupation of these M sites.¹⁷ As depicted in Figure 2, the [PbBi₃Te₆][−] slab can be viewed as a fragment excised from PbTe-type structure along the [011] direction with a thickness of four {PbTe} monolayers.

The structure of CsPb₂Bi₃Te₇ (**2**) has thicker [Pb₂Bi₃Te₇][−] slabs, Figure 1b. Interestingly, these slabs are also excised fragments from the PbTe structure with five {PbTe} monolayers, i.e., one monolayer thicker than the slab in **1**. As a result, the *b* axis, perpendicular to the layers, is correspondingly increased. There are some significant differences in the stacking and structural details of the slabs in the two compounds. First, as the slabs stack along

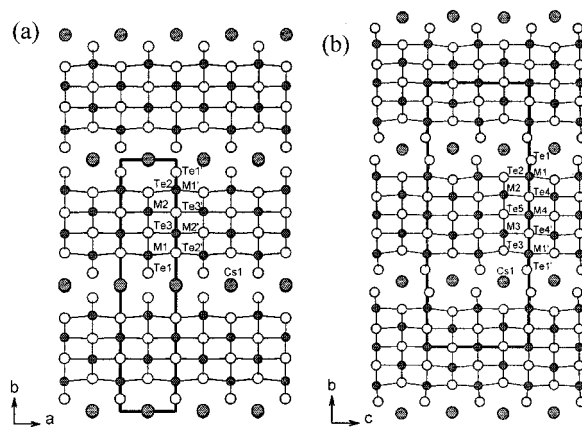


Figure 1. The structures of (a) CsPbBi₃Te₆ (**1**) and (b) CsPb₂Bi₃Te₇ (**2**) in projection. The large shaded circles are Cs atoms, small shaded circles are Pb/Bi atoms, and open circles are Te atoms. M(1), M(2), M(3), and M(4) are sites of mixed Pb/Bi occupation.

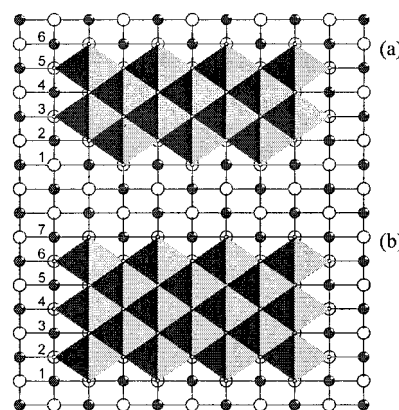


Figure 2. A perspective view of the PbTe structure along the [011] direction. The polyhedra represent the PbTe octahedra. (a) The [PbBi₃Te₆][−] slab in **1** as a fragment excised from this lattice (four monolayers thick counting from 2–5). (b) The [Pb₂Bi₃Te₇][−] slab in **2** as a fragment that is seven monolayers thick (five monolayers thick counting from 2–6).

the *b*-axis the rows of μ_2 -Te(1) atoms found on their surfaces are arranged in staggered fashion in **1**, but they are eclipsed in **2**. Second, the μ_2 -Te(1) atom shifts away from its *m2m* site in **1** to a *m* site in **2** causing the repeating unit along the *c* axis in **2** to double.

Since CsPbBi₃Te₆ and CsBi₄Te₆ possess a “M₄Te₆” type of framework, it is interesting to compare and contrast these two structures. CsBi₄Te₆ containing formally Bi²⁺ ions features distinct infinite [Bi₄Te₆][−] rods arranged side-by-side and linked with Bi–Bi bonds to make slabs.¹² As the Bi²⁺ ions are replaced by Pb²⁺ ions to give CsPbBi₃Te₆, Bi–Bi bonding is no longer possible, nor necessary. The [Bi₄Te₆][−] slabs (now [PbBi₃Te₆][−]) evolve, through

* Address correspondence to this author. E-mail: kanatzid@cem.msu.edu.

[†] Department of Chemistry and Center for Fundamental Materials Research.

[‡] Department of Electrical and Computer Engineering.

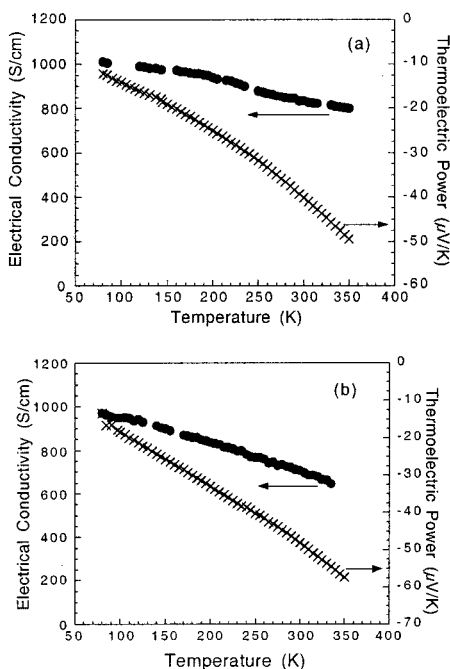


Figure 3. Variable-temperature electrical conductivity and thermopower data for oriented polycrystalline ingot samples of (a) CsPbBi₃Te₆ (**1**) and (b) CsPb₂Bi₃Te₇ (**2**). The crosses are thermopower.

cleavage of Bi–Bi bonds and formation of new Bi(Pb)–Te bonds, into the infinite slabs shown in Figure 1a.

In both structures, the Cs cations are surrounded by nine Te atoms with Cs–Te distances between 3.433(3) and 4.243(6) Å. The resulting tricapped trigonal prismatic environment is similar to that found in CsBi₄Te₆. Occupancy refinement of the Cs(1) sites showed 85% for **1** and 91% for **2**. Therefore, to maintain electroneutrality the final formulas were adjusted to be Bi-rich compositions; Cs_{1-x}Pb_{1-x}Bi_{3+x}Te₆ ($x = 0.15$) of **1** and Cs_{1-x}Pb_{2-x}Bi_{3+x}Te₇ ($x = 0.09$) of **2**. The isostructural Sn analogues gave similarly Cs-deficient stoichiometries.^{15,16}

Charge transport measurements on polycrystalline ingots of **1** and **2** show high electrical conductivity at room temperature, which increases as the temperature drops.

The conductivities decrease from 1010 S/cm at 80 K to 800 S/cm at 350 K for **1** and from 970 S/cm at 80 K to 570 S/cm at 350 K for **2**, Figure 3. The thermopower of **1** and **2** is -50 and -57 $\mu\text{V/K}$ at 350 K, respectively, rising to higher values with rising temperature. These conductivities are affected by the morphological defects (crack, grain boundaries, etc) of the ingots used. The intrinsic conductivities are probably much higher. The relatively low thermopower and metallic-like temperature dependence of conductivity of **1** and **2** indicate that both materials are heavily doped and are reminiscent of those of CsBi₄Te₆ before being optimized through doping. The negative sign of thermopower indicates n-type charge transport in these compounds. This is consistent with their Bi-rich nonstoichiometric nature suggested by the elemental analysis and crystallographic refinement. A Bi-rich/Pb-deficient stoichiometry will result in electron carrier excess in these materials giving rise to negative thermopower, as Bi possesses an extra electron compared to Pb. Presumably, a Pb-rich/Bi-deficient stoichiometry would lead to p-type behavior. The thermal conductivities at room temperature are very low at 1.8 W/(m·K) for **1** and 1.6 W/(m·K) for **2**, comparable to those of Bi₂Te₃ and CsBi₄Te₆.¹²

The new structure types reported here are able to form a number of other isostructural members (in addition to **3** and **4**) such as rubidium analogues and antimony CsPbSb₃Te₆ and CsPb₂Sb₃Te₇.

Consequently, the novel two-dimensional structures in these systems define two potentially promising adaptable platforms for thermoelectric investigations.

Acknowledgment. Financial support from ONR and DARPA is gratefully acknowledged.

Supporting Information Available: Tables of crystallographic details, atomic coordinates, bond lengths and angles, and anisotropic thermal parameters for all compounds (CIF). This material is available free of charge via the Internet at <http://pubs.acs.org>.

References

- (1) Slack, G. A. *New Materials and Performance Limits for Thermoelectric Cooling*. In *CRC Handbook of Thermoelectrics*; Rowe, D. M., Ed.; CRC Press: Boca Raton, FL, 1995; p 407. (b) Kanatzidis, M. G. *Semicond Semimet* **2000**, *69*, 51–100. (c) Mahan, G. D. Good thermoelectrics. In *Solid State Phys.* **1998**, *51*, 81. (d) DiSalvo, F. J. *Science* **1999**, *285*, 703.
- (2) Dresselhaus, M. S.; Dresselhaus, G.; Sun, X.; Zhang, Z.; Cronin, S. B.; Koga, T.; Ying, J. Y.; Chen, G. The promise of low-dimensional thermoelectric materials. In *Microscale Thermophys. Eng.* **1999**, *3*, 89.
- (3) Iordanidis, L.; Brazis, P. W.; Kyratsi, T.; Ireland, J.; Lane, M.; Kannewurf, C. R.; Chen, W.; Dyck, J. S.; Uher, C.; Ghelani, N. A.; Hogan, T.; Kanatzidis, M. G. *Chem. Mater.* **2001**, *13*, 622.
- (4) Choi, K. S.; Chung, D. Y.; Mrotzek, A.; Brazis, P.; Kannewurf, C. R.; Uher, C.; Chen, W.; Hogan, T.; Kanatzidis, M. G. *Chem. Mater.* **2001**, *13*, 756.
- (5) Wang, Y. C.; DiSalvo, F. J. *Chem. Mater.* **2000**, *12*, 1011.
- (6) Shelimova, L. E.; Karpinskii, O. G.; Zemskov, V. S.; Konstantinov, P. P. *Inorg. Mater.* **2000**, *36*, 235.
- (7) Chung, D. Y.; Lane, M. A.; Ireland, J. R.; Brazis, P. W.; Kannewurf, C. R.; Kanatzidis, M. G. *Mater. Res. Soc. Symp.* **2000**, *626*, 27.4.1.
- (8) Mrotzek, A.; Chung, D. Y.; Hogan, T.; Kanatzidis, M. G. *J. Mater. Chem.* **2000**, *10*, 1667.
- (9) Iordanidis, L.; Kanatzidis, M. G. *Angew. Chem., Int. Ed.* **2000**, *39*, 1927.
- (10) Oosawa, Y.; Tatenno, Y.; Mukaida, M.; Tsunoda, T.; Imai, Y.; Isoda, Y.; Nishida, I. A. *Proc. Inter. Conf. Thermoelect.* **1999**, 550.
- (11) Chung, D. Y.; Jobic, S.; Hogan, T.; Kannewurf, C. R.; Breck, R.; Rouxel, J.; Kanatzidis, M. G. *J. Am. Chem. Soc.* **1997**, *119*, 2505.
- (12) Chung, D. Y.; Hogan, T.; Brazis, P.; Rocci-Lane, M.; Kannewurf, C. R.; Bastea, M.; Uher, C.; Kanatzidis, M. G. *Science* **2000**, *287*, 1024.
- (13) CsPbBi₃Te₆ (**1**) was obtained by reacting CsBi₄Te₆ (0.252 g, 0.145 mmol), Pb (0.0301 g, 0.145 mmol), and Te (0.0186 g, 0.146 mmol) at 600 °C for 1 h and slow cooling to 50 °C. CsPb₂Bi₃Te₇ (**2**) was obtained by reacting CsBi₄Te₆ (0.203 g, 0.117 mmol), Pb (0.0728 g, 0.351 mmol), and Te (0.0448 g, 0.351 mmol) at the same heating profile with **1**. Both compounds can be prepared by the stoichiometric reactions of Cs₂Te, Pb, Bi, and Te reagents. A quantitative microprobe analysis using energy dispersive spectroscopy (EDS) on >10 crystals gave an average molar ratio of Cs:[Pb(Bi)]:Te of 0.86:[4.10]:6.14 for **1** and 0.95:[4.97]:7.3 for **2**. The microprobe analyses do indicate a Bi-rich composition.
- (14) Crystal data: (**1**), Cs_{0.85}Pb_{0.85}Bi_{3.15}Te₆, orthorhombic, space group *Cmcm*, black needlelike crystal, $a = 6.3322(6)$ Å, $b = 28.667(3)$ Å, $c = 4.3637(4)$ Å, $T = 273$ K, $V = 792.1(2)$ Å³, $Z = 4$, final refinement converged to $R_1(F) = 0.0391$, $wR_2(F^2) = 0.1049$. (**2**), Cs_{0.91}Pb_{1.9}Bi_{3.09}Te₇, orthorhombic, *Cmcm*, black needlelike crystal, $a = 4.3456(6)$ Å, $b = 32.476(5)$ Å, $c = 12.508(2)$ Å, $T = 273$ K, $V = 1765.2(7)$ Å³, $Z = 8$, final $R_1(F) = 0.0410$, $wR_2(F^2) = 0.1131$, GOF = 1.062. The metal sites in both structures were refined as Bi atoms due to the nearly identical scattering lengths of Pb and Bi.
- (15) CsSnBi₃Te₆ (**3**) was obtained by reacting CsBi₄Te₆ (0.301 g, 0.173 mmol), Sn (0.0206 g, 0.173 mmol), and Te (0.0221 g, 0.173 mmol) at 750 °C for 1 h and slow cooling to 50 °C. CsSn₂Bi₃Te₇ (**4**) was obtained by reacting CsBi₄Te₆ (0.302 g, 0.174 mmol), Sn (0.0620 g, 0.522 mmol), and Te (0.0667 g, 0.523 mmol) at the same heating profile with **3**. Both compounds can be prepared by the stoichiometric reactions of Cs₂Te, Sn, Bi, and Te reagents. EDS analysis on several crystals gave an average composition of Cs_{0.87}Sn_{0.73}Bi_{3.30}Te_{6.25} for **3** and Cs_{0.93}Sn_{1.82}Bi_{3.25}Te_{7.20} for **4**.
- (16) Crystal data: (**3**), Cs_{0.84}Sn_{0.84}Bi_{3.16}Te₆, *Cmcm*, black needlelike crystal, $a = 6.2613(7)$ Å, $b = 28.479(3)$ Å, $c = 4.3207(5)$ Å, $T = 273$ K, $V = 770.4(3)$ Å³, $Z = 4$, final refinement converged to $R_1(F) = 0.0467$, $wR_2(F^2) = 0.1358$, GOF = 1.213. (**4**), Cs_{0.88}Sn_{1.88}Bi_{3.12}Te₇, *Cmcm*, $a = 4.3881(6)$ Å, $b = 33.139(4)$ Å, $c = 12.608(2)$ Å, $T = 273$ K, $V = 1833.4(7)$ Å³, $Z = 8$, final $R_1(F) = 0.0353$, $wR_2(F^2) = 0.0872$. The refinements of metal sites in **3** showed 18.0(4)% Sn occupancy in the Bi(1) site and 24.0(4)% in the Bi(2) site. The refinements of metal sites in **4** showed 23.4(2)% Sn in the Bi(1) site, 50.8(4)% Sn in the Bi(2) site, 41.2(4)% Sn in the Bi(3) site, and 49.6(4)% Sn in the Bi(4) site. The final formulas of **3** and **4** were adjusted to be Cs_{1-x}Sn_{1-x}Bi_{3+x}Te₆ ($x = 0.16$) and Cs_{1-x}Sn_{2-x}Bi_{3+x}Te₇ ($x = 0.12$), respectively.
- (17) As suggested by valence bond sum calculations, both Pb²⁺ and Bi³⁺ ions appear to occupy the two metal sites. Brown, I. D. *J. Appl. Crystallogr.* **1996**, *29*, 479.

JA017602I